BIOCHEMISTRY
including biophysical chemistry & molecular biology

ARTICLE

pubs.acs.org/biochemistry

Lung Surfactant Protein A (SP-A) Interactions with Model Lung Surfactant Lipids and an SP-B Fragment

Muzaddid Sarker,[†] Donna Jackman,[‡] and Valerie Booth[*,†,‡]

[†]Department of Physics and Physical Oceanography and [‡]Department of Biochemistry, Memorial University of Newfoundland, St. John's, NL, Canada

Supporting Information

ABSTRACT: Surfactant protein A (SP-A) is the most abundant protein component of lung surfactant, a complex mixture of proteins and lipids. SP-A performs host defense activities and modulates the biophysical properties of surfactant in concerted action with surfactant protein B (SP-B). Current models of lung surfactant mechanism generally assume SP-A functions in its octadecameric form. However, one of the findings of this study is that when SP-A is bound to detergent and lipid micelles that mimic lung surfactant phospholipids, it exists predominantly as smaller oligomers, in sharp contrast to the much larger forms observed when alone in water. These investigations were carried out in sodium dodecyl sulfate (SDS), dodecylphosphocholine (DPC), lysomyristoylphosphatidylcholine (LMPC), lysomyristoylphosphatidylglycerol (LMPG), and mixed LMPC + LMPG micelles, using solution and diffusion nuclear magnetic resonance (NMR) spectroscopy. We have also probed SP-A's interaction with Mini-B, a biologically active synthetic fragment of SP-B, in the presence of micelles. Despite variations in Mini-B's own interactions with micelles of different compositions, SP-A is found to interact with Mini-B in all micelle systems and perhaps to undergo a further structural rearrangement upon interacting with Mini-B. The degree of SP-A−Mini-B interaction appears to be dependent on the type of lipid headgroup and is likely mediated through the micelles, rather than direct binding.

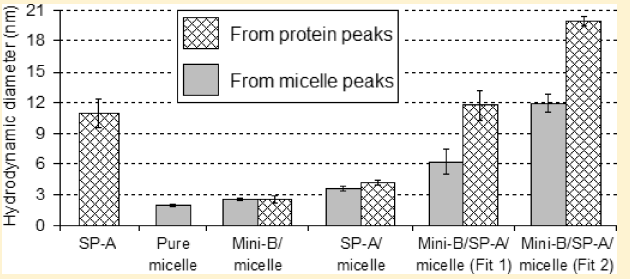

Lung surfactant is a mixture of lipids and proteins that enables normal breathing by reducing the surface tension at the air−water interface in alveoli and additionally provides the first line of defense against inhaled microbes in the lungs. Surfactant protein A (SP-A) is the most abundant protein component of the lung surfactant system.[1] Substantial evidence indicates that SP-A is a major contributor to innate host defense and inflammatory immunomodulator processes of the lung.[2−7] SP-A may also play a role in the surface activity of lung surfactant. For instance, SP-A is essential for the formation of tubular myelin,[8] a potential structural precursor to the surface-active film. SP-A also enhances adsorption of phospholipids along the air−water interface in concerted action with surfactant protein B (SP-B)[9,10] and induces calcium-dependent aggregation of lipid vesicles with or without SP-B or surfactant protein C (SP-C).[11,12] Furthermore, SP-A has been shown to improve the surface activity of surfactant under several challenging conditions such as the low surfactant concentrations[13] and the presence of inhibitory plasma proteins[14] or oxidants.[15]

SP-A is a multimeric glycoprotein. The capabilities of SP-A to bind surfactant phospholipids, pathogen-associated molecular patterns, and receptors on cell surfaces likely depend on its complex oligomeric structure.[16] SP-A can assemble as a hexamer of trimeric subunits; i.e., a total of 18 SP-A molecules may join together to form the quaternary structure. This octadecameric conformation is generally assumed to be the form in which the protein carries out its biological functions.[2,17]

SP-A's primary structure is highly conserved among different mammalian species.[18] A single chain of human SP-A consists of 248 amino acids, as does the bovine SP-A used in this work.[19] Its molecular weight varies from organism to organism, from ∼28 to 36 kDa depending on the extent of post-translational modifications (e.g., glycosylation).[20] SP-A belongs to the structurally homologous family of innate immune defense proteins known as collectins, so named for their collagen-like and lectin domains.[17] It possesses four structural domains: a short N-terminal domain that contains the cysteines required for intermolecular disulfide bond formation, a proline-rich collagen-like domain that is important for oligomerization, an α-helical coiled-coil neck domain that is involved in trimerization, and a globular C-terminal carbohydrate recognition domain (CRD).[2,17,21] The high-resolution crystal structures of recombinant trimeric CRD and neck domains of rat SP-A, in both native and ligand-bound forms, have been determined (PDB IDs 1R13 and 1R14),[22] but the complete structures of the full protein, its glycosylated form, or higher oligomers are still unavailable.

SP-A is a hydrophilic and hence water-soluble protein. However, in the lungs, only about 10% of the total SP-A population is found in the aqueous phase and almost 90% is lipid-associated, the bulk of which is present within tubular myelin.[23] Therefore,

Received: February 2, 2011
Revised: April 27, 2011
Published: May 09, 2011

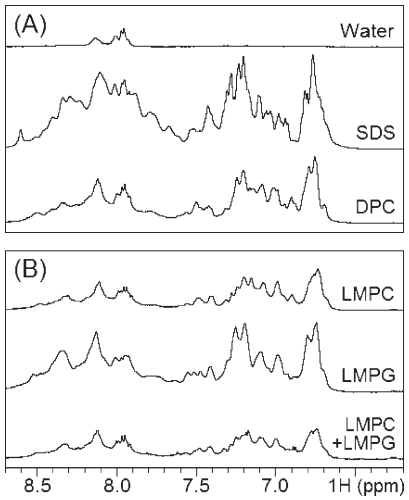

Figure 1. HN regions of 1D ^{1}H NMR spectra of SP-A in water and in different micelle environments. (A) 0.2 mM SP-A in water and in 40 mM SDS and 40 mM DPC (256 scans). (B) 0.25 mM SP-A in 50 mM LMPC, 50 mM LMPG, and 42.5 mM LMPC + 7.5 mM LMPG (160 scans). All spectra within each panel are shown with the same intensity scale. However, the intensity scales are not comparable between the panels as sample compositions and acquisition parameters were different.

interactions with phospholipids likely play important roles in SP-A's biological function. We have thus performed solution and diffusion nuclear magnetic resonance (NMR) studies to investigate the lipid interactions and level of oligomerization of bovine SP-A, using an array of five different micelle systems mimicking various lipid components of lung surfactant. The investigation started with anionic sodium dodecyl sulfate (SDS) and zwitterionic dodecylphosphocholine (DPC) micelles that are routinely used in solution NMR studies of lipid-associated or membrane proteins. It then proceeded to more physiologically relevant micelle mimetics constituted from lysomyristoylphosphatidylcholine (LMPC), a single chain analogue of the surfactant phospholipids containing the zwitterionic PC headgroup, and lysomyristoylphosphatidylglycerol (LMPG), a single chain analogue of the surfactant phospholipids containing the anionic PG headgroup. Finally, a mixed LMPC (85%) + LMPG (15%) micelle system was used approximating the physiological ratio of PC to PG.

We have also used NMR techniques to probe the interaction of SP-A with Mini-B in all these micelle systems. Mini-B is a synthetic construct comprising the N- and C-terminal helices of SP-B. Measurements of blood oxygenation and dynamic lung compliance of surfactant deficient rat models show that Mini-B performs as well as the full-length protein.[24] Thus, Mini-B likely encompasses the key functional regions of SP-B. SP-B itself is essential for lung surfactant function.[25,26] There are several indications of interaction, either direct or indirect, between SP-A and SP-B. Although SP-A is not strictly required for the biophysical function of lung surfactant,[27] it improves the surface activity of lipid−protein preparations only if SP-B is present, especially in the presence of anionic phospholipids.[9,28] The synergy between SP-A and SP-B observed in the process of phospholipid membrane fusion has been attributed to specific calcium-dependent interactions between them.[29,30] Likewise, the perturbation of dipalmitoylphosphatidylcholine (DPPC)/dipalmitoylphosphatidylglycerol (DPPG) bilayers by SP-A and SP-B together is different from the sum of the effects of the individual proteins.[31] The proteins also demonstrate a cooperative calcium-dependent action in improving the resistance to surfactant inhibition by blood and plasma proteins.[32] However, the most dramatic exhibition of a concerted action is probably the *in vitro* reconstitution of tubular myelin when SP-A and SP-B are added to the mixtures of DPPC and PG in the presence of calcium.[33−35] Knowledge of the high-resolution structure of Mini-B,[36] along with its NMR chemical shifts, provided an opportunity to directly probe SP-A−Mini-B interactions in the presence of model lipids.

Solution NMR techniques are frequently employed in probing protein−protein interactions due to the sensitivity of NMR chemical shift to the surrounding environment which allows the binding surface of a protein to be mapped, merely by titrating in its binding partner and tracking the changes in the position and/or intensity of the NMR signals.[37] However, there were some additional complexities involved in applying this strategy to study the SP-A−Mini-B interaction. First, SP-A octadecamers are about 504−648 kDa and thus very large for solution NMR and are expected to give very broad, weak peaks in the spectra. Second, since the hydrophobic Mini-B was solubilized in SDS micelles for the structural studies, it was necessary to characterize Mini-B's own interactions with various micelles in addition to SP-A−micelle interactions before investigating any SP-A−Mini-B interaction in the presence of those micelles.

MATERIALS AND METHODS

Protein Preparation. SP-A was isolated and purified from cow lungs, as described elsewhere.[38,39] The molecular mass of SP-A (29.022 KDa) was confirmed by SDS−polyacrylamide gel electrophoresis (SDS-PAGE) and matrix-assisted laser desorption/ionization−time-of-flight (MALDI-TOF) mass spectrometry. Mini-B was produced by solid phase chemical synthesis employing *O*-fluorenylmethyloxycarbonyl (Fmoc) chemistry and purified by preparative reverse phase high performance liquid chromatography (HPLC), as described elsewhere.[36] The 34-residue Mini-B possessed 9 backbone ^{15}N-labeled amino acids: 6 leucines at positions 3, 7, 22, 25, 29, and 31, 2 alanines at positions 6 and 13, and 1 glycine at position 18.

NMR Sample Preparation. SP-A samples were prepared in aqueous solution (90% H_2O + 10% D_2O) containing 0.4 mM 2,2-dimethyl-2-silapentane-5-sulfonate (DSS), 0.2 mM NaN_3, and 4.5 mM Hepes. SP-A−micelle samples were prepared by adding the required amounts of detergents/lipids to the aqueous sample. At least two samples were prepared for each micelle system with differing ratios of the protein to detergent/lipid. However, for each sample, the molar concentration of the detergent/lipid was kept at least 200 times higher than the monomeric concentration of SP-A. The exact protein and detergent/lipid concentrations of the samples are mentioned in the captions of Figures 1−4. For SDS and DPC samples, deuterated (98%) detergents, purchased from Cambridge Isotope Laboratories (Andover, MA), were used. For LMPC and LMPG samples, nondeuterated lipids, purchased from Avanti Polar Lipids (Alabaster, AL), were used as their deuterated versions were not commercially available. The samples were set to pH 6.9 using NaOH and HCl solutions. Mini-B samples were prepared separately, maintaining identical conditions to the SP-A samples. Finally, SP-A and Mini-B samples in each micelle system were mixed together at equal quantities (i.e., a protein monomer ratio of 1 to 1) to prepare the mixed protein samples.

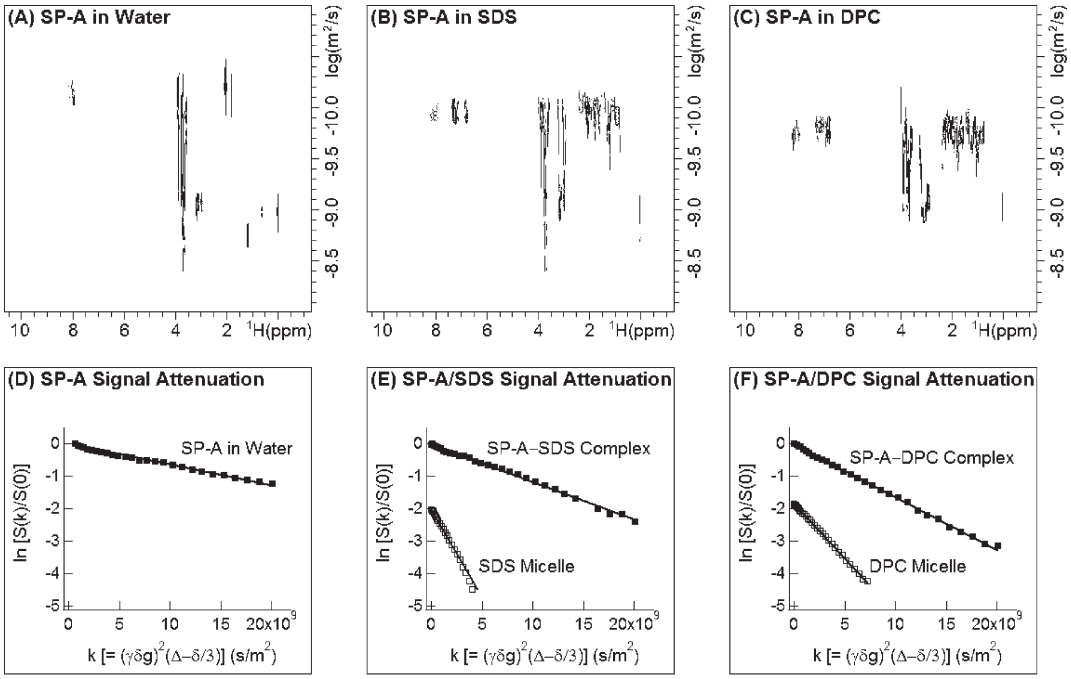

Figure 2. Translational diffusion measurements of SP-A in water, SDS, and DPC micelles. Top panels show the 2D DOSY spectra of 0.2 mM SP-A in water (A), 0.2 mM SP-A in 40 mM SDS (B), and 0.2 mM SP-A in 40 mM DPC (C). Bottom panels show the linear fits obtained for the attenuation of the integrated HN region of SP-A in water (D), in complex with SDS (E), and in complex with DPC (F). The linear fits for pure SDS (40 mM) and DPC (40 mM) micelles, obtained from the attenuation of the peak at 0.80 ppm, are included in (E) and (F) for comparison.

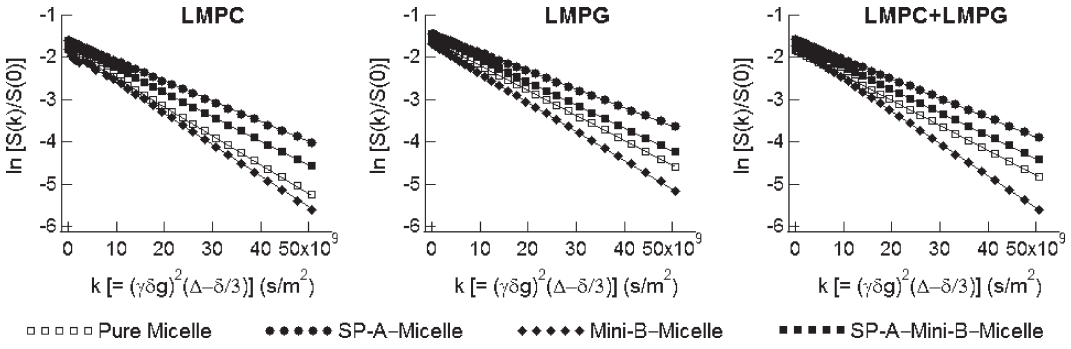

Figure 3. Translational diffusion measurements of SP-A and Mini-B in LMPC, LMPG, and LMPC (85%) + LMPG (15%) micelle systems. 2D DOSY data were acquired separately for pure micelles (50 mM), SP-A (0.25 mM) in micelles (50 mM), Mini-B (0.25 mM) in micelles (50 mM), and SP-A (0.125 mM) + Mini-B (0.125 mM) in micelles (50 mM). Linear fits show the attenuation of the ^{1}H signals for micelles and protein−micelle complexes as determined from the lipid peak at 0.86 ppm.

Collection and Processing of Solution NMR Data. NMR spectra were acquired on a Bruker Avance II 14.1 T (600 MHz) spectrometer (Billerica, MA) using an inverse triple resonance TXI probe. Data were collected and processed using Bruker Topspin 2.0. 1D ^{1}H experiments were performed for SP-A in water, SP-A−micelle, Mini-B−micelle, and SP-A−Mini-B−micelle systems. 2D ^{15}N−^{1}H HSQC experiments were performed for the samples containing Mini-B. All experiments were performed at 37 °C to match the physiological temperature. 1D ^{1}H spectra were acquired with 128−320 scans using the water-gate water suppression technique[40] and processed using an exponential apodization function with 1 Hz line broadening. 2D ^{15}N−^{1}H HSQC spectra were acquired with 160−320 scans using the flip-back water suppression technique[41] and processed using the Qsine apodization function with a sine bell shift of 2. Although the NMR experiments were performed for at least two separately prepared samples of each system, spectra of both samples essentially looked identical.

Collection and Processing of Diffusion NMR Data. Diffusion-ordered spectroscopy (DOSY) experiments were performed on the same Bruker Avance II 14.1 T (600 MHz) spectrometer employing pulsed field gradient (PFG) NMR.[42] The pulse sequence used a stimulated echo with bipolar gradient pulses and one spoil gradient,[43] followed by a 3−9−19 pulse for water suppression.[44] The ^{1}H signals were attenuated to ∼5% of their initial amplitudes by increasing the gradient strength from ∼2% to 95% in 32 steps. Experiments were performed at 37 °C for SP-A in water and SDS and DPC samples, but at 25 °C for LMPC,

dx.doi.org/10.1021/bi200167d |*Biochemistry* 2011, 50, 4867–4876

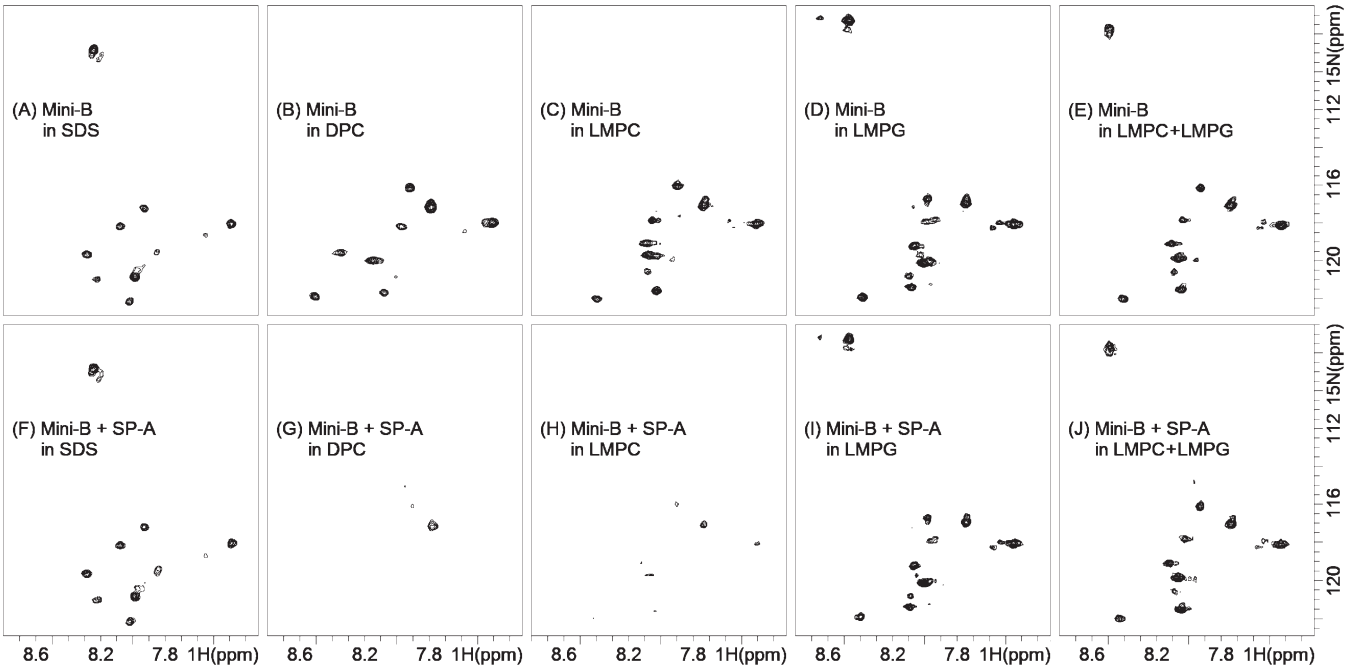

Figure 4. 2D $^{15}N-^{1}H$ HSQC spectra of Mini-B in different micelles in the absence (top panels) and presence (bottom panels) of SP-A. 0.2 mM Mini-B (A) and 0.1 mM Mini-B + 0.1 mM SP-A (F) in 40 mM SDS. 0.2 mM Mini-B (B) and 0.1 mM Mini-B + 0.1 mM SP-A (G) in 40 mM DPC. 0.25 mM Mini-B (C) and 0.125 mM Mini-B + 0.125 mM SP-A (H) in 50 mM LMPC. 0.25 mM Mini-B (D) and 0.125 mM Mini-B + 0.125 mM SP-A (I) in 50 mM LMPG. 0.25 mM Mini-B (E) and 0.125 mM Mini-B + 0.125 mM SP-A (J) in 42.5 mM LMPC + 7.5 mM LMPG. Spectra A−E were acquired using 160 scans, and spectra F−J were acquired using 320 scans.

LMPG, and LMPC + LMPG samples to minimize the effect of thermal convection. The pseudo 2D DOSY spectra were produced using Bruker Topspin 2.0. The integrated signal intensities were exported to Igor Pro for curve fitting. The translational diffusion coefficient, D_C, was derived from the 1D ^{1}H experiments underlying the 2D DOSY, using the equation for the attenuation of signal

$$\ln[S(k)/S(0)] = -D_C k$$

with

$$k = \gamma^2 g^2 \delta^2 (\Delta - \delta/3)$$

where $S(k)$ is the observed signal intensity, $S(0)$ is the unattenuated signal intensity, γ is the gyromagnetic ratio of the observed nucleus (^{1}H), g is the gradient strength (maximum amplitude 35 G/cm), δ is the gradient pulse length (optimized between 3 and 8 ms), and Δ is the diffusion time (100 ms). The diffusion coefficient was determined from the slope of the linear fit for $\ln[S(k)/S(0)]$ versus k. The observed diffusion coefficient, D_C, was converted into apparent hydrodynamic diameter, d_{HA}, using the Stokes−Einstein equation

$$D_C = k_B T/3\pi\eta d_{HA}$$

where k_B is the Boltzmann constant, T is the absolute temperature, and η is the viscosity of the solution (8.91×10^{-4} kg/(m s) at 25 °C or 6.92×10^{-4} kg/(m s) at 37 °C).

For each system, translational diffusion measurements were performed using multiple peaks, and the average value of D_C, and corresponding d_{HA}, was determined. In deuterated SDS and DPC micelles, two separate values of average D_C and d_{HA} were calculated from the attenuation of detergent peaks at 0.80 and 1.22 ppm and protein peaks at 0.92 ppm and the integrated HN region. However, in nondeuterated LMPC, LMPG, and LMPC + LMPG micelles, the signals from the lipids overwhelmed the signals from the protein, and so, the average D_C and d_{HA} for these systems were calculated from the lipid peaks only. Four LMPC/LMPG peaks at 0.86, 1.28, 1.59, and 2.37 ppm were used. For SP-A in water, the average D_C and d_{HA} were calculated using the peak at 2.03 ppm and the integrated HN region.

For SDS and DPC samples, because the diffusion measurements were obtained from the protein peaks in addition to the detergent peaks, the subpopulations of protein−micelle complexes, $S_{complex}$, and protein−free micelles, $S_{micelle}$ (= $1 - S_{complex}$) (Supporting Information, Table S1), were determined using a two-site model[45]

$$D_{C(observed)} = S_{complex} D_{C(complex)} + (1 - S_{complex}) D_{C(micelle)}$$

where $D_{C(observed)}$ is the observed diffusion coefficient of the protein−micelle sample and $D_{C(complex)}$ and $D_{C(micelle)}$ are the diffusion coefficients of the protein−micelle complexes and pure micelles, respectively.

RESULTS

SP-A−Micelle Interactions. 1D ^{1}H spectra of SP-A in water and in different micelle environments were acquired to obtain indications of the protein conformation. Figure 1 shows the HN regions (6.2−8.7 ppm) of 1D ^{1}H spectra of SP-A in water and in different micelle environments. In water, very few signals are observed, and those are broad and weak, as expected for a high molecular mass protein. The few observable signals are likely generated by some highly mobile region(s) of SP-A undergoing fast motion (e.g., a flexible loop). Interestingly, drastic changes in the SP-A spectra are observed with the addition of detergent or

Table 1. Average Observed Translational Diffusion Coefficients and Corresponding Apparent Hydrodynamic Diameters of Detergent/Lipid Micelles and Protein−Micelle Complexes As Calculated from the DOSY Signal Attenuation

composition	peaks from	observed diffusion coefficient $\times 10^{-10}$ (m^2/s)	apparent hydrodynamic diameter (nm)
SP-A in water	SP-A	0.596 ± 0.079	11.11 ± 1.48
SDS micelles	SDS	5.395 ± 0.101	1.22 ± 0.02
SP-A−SDS complex	SDS	2.091 ± 0.595	3.27 ± 0.93
	SP-A	1.055 ± 0.158	6.30 ± 0.94
Mini-B−SDS complex	SDS	3.460 ± 0.052	1.90 ± 0.03
	Mini-B	2.696 ± 0.267	2.45 ± 0.25
SP-A−Mini-B−SDS complex: fit 1	SDS	1.661 ± 0.072	3.95 ± 0.17
	protein	0.993 ± 0.041	6.61 ± 0.27
SP-A−Mini-B−SDS complex: fit 2	SDS	0.501 ± 0.028	13.12 ± 0.74
	protein	0.328 ± 0.014	20.02 ± 0.86
DPC micelles	DPC	3.362 ± 0.008	1.96 ± 0.01
SP-A−DPC complex	DPC	1.837 ± 0.110	3.57 ± 0.21
	SP-A	1.566 ± 0.077	4.20 ± 0.21
Mini-B−DPC complex	DPC	2.621 ± 0.051	2.51 ± 0.04
	Mini-B	2.591 ± 0.359	2.56 ± 0.35
SP-A−Mini-B−DPC complex: fit 1	DPC	1.068 ± 0.206	6.26 ± 1.21
	protein	0.561 ± 0.070	11.80 ± 1.48
SP-A−Mini-B−DPC complex: fit 2	DPC	0.549 ± 0.037	11.99 ± 082
	protein	0.327 ± 0.007	20.07 ± 0.43
LMPC micelles	LMPC	0.671 ± 0.009	7.30 ± 0.10
SP-A−LMPC complex	LMPC	0.472 ± 0.009	10.37 ± 0.21
Mini-B−LMPC complex	LMPC	0.737 ± 0.002	6.65 ± 0.02
SP-A−Mini-B−LMPC complex	LMPC	0.572 ± 0.008	8.56 ± 0.11
LMPG micelles	LMPG	0.589 ± 0.002	8.31 ± 0.03
SP-A−LMPG complex	LMPG	0.435 ± 0.003	11.27 ± 0.08
Mini-B−LMPG complex	LMPG	0.682 ± 0.005	7.18 ± 0.05
SP-A−Mini-B−LMPG complex	LMPG	0.537 ± 0.007	9.13 ± 0.12
LMPC+LMPG micelles	LMPC+LMPG	0.583 ± 0.009	8.40 ± 0.13
SP-A−LMPC+LMPG complex	LMPC+LMPG	0.452 ± 0.009	10.83 ± 0.22
Mini-B−LMPC+LMPG complex	LMPC+LMPG	0.745 ± 0.022	6.57 ± 0.20
SP-A−Mini-B−LMPC+LMPG complex	LMPC+LMPG	0.538 ± 0.009	9.10 ± 0.15

lipid micelles. The HN regions display many intense and dispersed signals consistent with a substantially lower SP-A molecular mass than observed in the absence of micelles.

To address this apparently substantial change of the SP-A oligomerization state upon addition of micelles, 2D DOSY experiments were performed to estimate the size of the complexes (Figures 2 and 3, Table 1). For SP-A alone in water, the apparent hydrodynamic diameter, d_{HA}, is 11.11 ± 1.48 nm. By contrast, the d_{HA} of SP-A−micelle complexes are much smaller in SDS and DPC. For SP-A−SDS, the d_{HA} are 3.27 ± 0.93 and 6.30 ± 0.94 nm, as measured using the SDS peaks and SP-A peaks, respectively. Similarly, for SP-A−DPC, the d_{HA} measured from the DPC peaks and SP-A peaks are 3.57 ± 0.21 and 4.20 ± 0.21 nm, respectively. The d_{HA} of pure micelles were also measured for comparison and found to be 1.22 ± 0.02 nm for SDS and 1.96 ± 0.01 for DPC, which conform well to what has been found by others for low SDS concentrations.[46] It is normal to obtain different diffusion coefficients from the detergent or lipid peaks compared to the protein peaks of a protein−micelle sample, since the observed value is the weighted average of the free and bound species.[47] And, this allows for the calculation of the relative populations of free and protein-bound micelles. On the basis of the application of a two-site model (Supporting Information, Table S1),[45] it is found that 76% of the SDS micelles and 85% of the DPC micelles are bound to SP-A, while the rest remain as protein-free micelles.

Translational diffusion measurements of the more physiologically relevant micelle systems indicate d_{HA} of 7.30 ± 0.10, 8.31 ± 0.03, and 8.40 ± 0.13 nm for LMPC, LMPG, and LMPC+LMPG micelles, respectively. When these micelles are bound to SP-A, the d_{HA} of the complexes are increased to 10.37 ± 0.21, 11.27 ± 0.08, and 10.83 ± 0.22 nm, respectively, as measured using the same lipid peaks. These d_{HA} are still substantially smaller than what would be expected for an octadecameric SP-A−micelle complex (Supporting Information, Table S2).

The effects of the interaction with micelles on the oligomeric state of SP-A were also supported by the results of a nonreducing SDS-PAGE (data not shown). No band was visible for SP-A in water, indicating a protein mass too large to enter the separating gel (i.e., >100 kDa). In DPC, a band at ∼60 kDa was seen, corresponding to the mass of an SP-A dimer. And in SDS, a band at ∼28 kDa was seen, corresponding to the mass of an SP-A monomer.

Mini-B−Micelle Interactions. Unlike SP-A, Mini-B was not soluble in water, and hence no experiments with Mini-B in the absence of micelles were possible. However, like SP-A, Mini-B also modifies the diffusion coefficients of all the micelle types

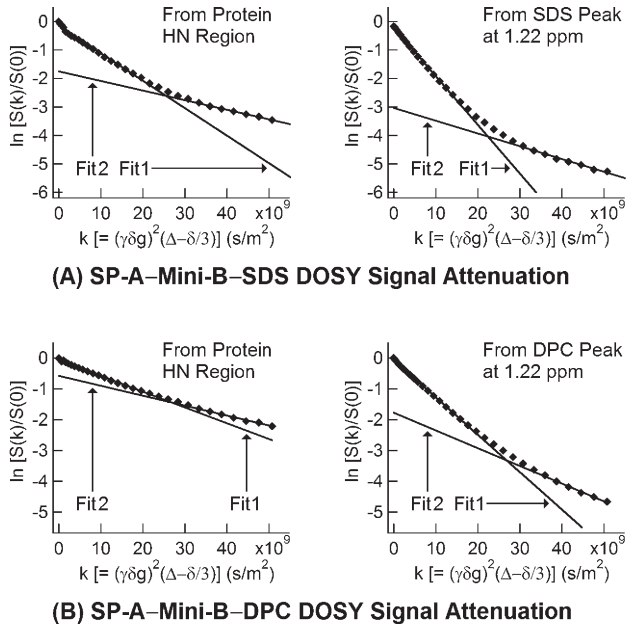

Figure 5. Signal attenuation curves obtained from the translational diffusion measurements of 0.1 mM SP-A + 0.1 mM Mini-B in 40 mM SDS (A) and in 40 mM DPC (B). None of the curves fit well with a single line. However, approximately the first and the last halves of the data fit well with two lines having two different slopes. Consequently, two diffusion coefficients are obtained for each system.

(Table 1), although, interesting differences are found between how Mini-B interacts with SDS/DPC detergent micelles versus LMPC/LMPG lipid micelles. The d_{HA} of the complex, upon inclusion of Mini-B, increases in detergent micelles but decreases in lipid micelles. While the d_{HA} of the SDS micelle is 1.22 ± 0.02 nm, that for the Mini-B−SDS complex increases to 1.90 ± 0.03 and 2.45 ± 0.25 nm when calculated from the SDS and Mini-B peaks, respectively. Similarly, the d_{HA} of the DPC micelle is 1.96 ± 0.01 nm, but this increases to 2.51 ± 0.04 and 2.56 ± 0.35 nm for the Mini-B−DPC complex when calculated from the DPC and Mini-B peaks, respectively. On the other hand, the d_{HA} of LMPC, LMPG, and LMPC+LMPG micelles are 7.30 ± 0.10, 8.31 ± 0.03, and 8.40 ± 0.13 nm, respectively, but upon inclusion of Mini-B, the d_{HA} of the peptide−micelle complexes decrease to 6.65 ± 0.02, 7.18 ± 0.05, and 6.57 ± 0.20 nm, respectively. Estimation of subpopulations, based on the two-site model (Supporting Information, Table S1), indicates that 72% of the SDS micelles and 96% of the DPC micelles are in complex with Mini-B, while the remainder exist as protein-free micelles.

1D ^{1}H and 2D ^{15}N−^{1}H HSQC spectra of Mini-B were acquired to obtain indications of peptide conformation in the micelle systems. The 6−9 ppm regions of 1D ^{1}H spectra of Mini-B display well-dispersed HN signals for all micelle compositions (not shown). However, 2D ^{15}N−^{1}H HSQC spectra indicate differences in Mini-B's conformation in anionic versus zwitterionic micelles as well as detergent versus lipid micelles (Figure 4A−E). All nine HSQC peaks are seen in SDS and LMPG micelles, but the peak for Gly18 (assigned in ref 36) is missing in DPC and LMPC micelles. Interestingly, in LMPC+LMPG micelles, the Gly18 peak is present, although the mixed micelles contain only 15% LMPG. There are several additional weak peaks present for Mini-B in LMPC, LMPG, and LMPC+LMPG but only a few in SDS and DPC, indicating greater conformational heterogeneity in the lipid versus detergent micelles.

SP-A−Mini-B Interactions. Experiments to probe any interaction between SP-A and Mini-B in the presence of micelles were performed using mixtures containing equimolar monomeric concentrations of each protein. 1D ^{1}H spectra of Mini-B−SP-A mixtures (not shown) look almost identical to that of SP-A alone. This is not unexpected as SP-A has more than 7 times as many amino acids as Mini-B.

Figure 4F−J displays the ^{15}N−^{1}H HSQC spectra of Mini-B after the addition of SP-A. In anionic and mixed micelles, all nine mini-B peaks, and the additional weaker peaks, remain unaffected by the inclusion of SP-A. In zwitterionic micelles, however, almost all Mini-B peaks disappear when SP-A is present, leaving very weak traces of only a few. This likely indicates that all or most of Mini-B are bound in complexes, presumably complexes of SP-A−micelle, which are too large to yield the HSQC signals. Since there is enough detergent/lipid present to provide more than twice as many zwitterionic micelles as Mini-B molecules, it seems that Mini-B has a strong preference to interact with SP-A−micelle complexes over micelles without SP-A. This interpretation is further supported by the absence of any changes to the missing or weak HSQC peaks of Mini-B even when extra DPC is added (not shown).

Since 2D HSQC spectra suggested that, upon addition of SP-A, there was likely a substantial increase in the size of Mini-B complexes in zwitterionic micelles but no major change in anionic or mixed micelles, we performed translational diffusion measurements to probe the change in size for all systems. Interestingly, 2D DOSY spectra of the SP-A−Mini-B mixture, when compared to that of the individual proteins, demonstrate a change in d_{HA} for all micelle compositions. As shown in Figure 5, the signal attenuation curves for SP-A−Mini-B mixtures in SDS and DPC micelles do not fit well with a single line (i.e., a single component fit). However, approximately the first and the last halves of the data are fit well with two lines having two different slopes [i.e., a two-component fit[48]]. Thus, two diffusion coefficients are obtained, and there are, at least, two distinct subpopulations of protein−micelle complexes present in the sample. The diffusion coefficients and corresponding hydrodynamic diameters measured from the two fits are reported in Table 1. In SDS, the d_{HA} of the SP-A−Mini-B subpopulations are 6.61 ± 0.27 and 20.02 ± 0.86 nm, as measured from the protein peaks. Although the d_{HA} of the first subpopulation is not significantly different from the SP-A−SDS complex (6.30 ± 0.94 nm), that of the second subpopulation is much larger. Hence, a fraction of the total Mini-B and SP-A molecules present in the mixture likely form large combined protein−micelle complexes. The approximate ratio of the small-to-large subpopulations of Mini-B−SP-A−SDS is 85%:15%, as estimated from the *y*-axis (relative signal intensity) intercepts of the two linear fits for the HN signal attenuation. In DPC, on the other hand, the d_{HA} of the SP-A−Mini-B subpopulations are 11.80 ± 1.48 and 20.07 ± 0.43 nm as measured from the protein peaks. In this case, the d_{HA} of both subpopulations are much larger than that of SP-A−DPC (4.20 ± 0.21 nm) or Mini-B−DPC (2.56 ± 0.35 nm) complexes. The approximate ratio of small-to-large subpopulations of Mini-B−SP-A−DPC is 62%:38%, as estimated from the *y*-axis intercepts of the two linear fits for the HN signal attenuation. Thus, in DPC, perhaps the entire populations of SP-A and Mini-B interact to form larger complexes, but with heterogeneous sizes.

Interestingly, the translational diffusion measurements in LMPC, LMPG, and LMPC+LMPG micelles demonstrate quite

different results from SDS and DPC micelles (Table 1). First, each of the signal attenuation curves for SP-A−Mini-B−micelle constitutes a single linear fit and hence yields a single diffusion coefficient. Thus, complexes with only a single homogeneous hydrodynamic diameter are apparently present for SP-A−Mini-B in LMPC, LMPG, and LMPC+LMPG systems. Second, the d_{HA} of SP-A−Mini-B−micelle complexes are larger than Mini-B−micelle complexes but, surprisingly, smaller than SP-A−micelle complexes. The d_{HA} of SP-A−Mini-B−LMPC is 8.56 ± 0.11 nm as opposed to 6.65 ± 0.02 nm for Mini-B−LMPC and 10.37 ± 0.21 nm for SP-A−LMPC. Similarly, the d_{HA} of SP-A−Mini-B−LMPG is 9.13 ± 0.12 nm, but that of Mini-B−LMPG is 7.18 ± 0.05 nm and SP-A−LMPG is 11.27 ± 0.08 nm. Also in mixed micelles, the d_{HA} are 9.10 ± 0.15 nm for SP-A−Mini-B−LMPC+LMPG, 6.57 ± 0.20 for Mini-B−LMPC+LMPG, and 10.83 ± 0.22 nm for SP-A−LMPC+LMPG.

To check if the observed micelle-bound SP-A represents most of the protein population or if there might be a significant fraction of the SP-A molecules not giving rise to observable signals, we performed a comparison between SP-A and Mini-B signal intensities in all micelle systems (Supporting Information, Table S3). When the tallest peaks in the HN regions, normalized with respect to DSS peak intensity, are compared, SP-A exhibits higher signal intensity than Mini-B by 22 times in SDS, 8 times in DPC, 6 times in LMPC, 5 times in LMPG, and 4 times in LMPC+LMPG. Thus, since all or most of the micelle-bound Mini-B is likely visible in the NMR spectra, most of the SP-A in the micelle samples is also likely being observed, at least in the absence of Mini-B. On the other hand, mixed SP-A−Mini-B exhibits 8, 4, 4, 2, and 2 times higher signal intensity, respectively, in the five micelle systems, when compared to Mini-B. Thus, in the mixed protein samples, significant fractions of the total populations appear to be absent from the spectra, presumably because their complexes are too large to observe by solution NMR. These large complexes are likely formed by interaction between SP-A and Mini-B.

DISCUSSION

Our initial NMR studies aimed at characterizing SP-A−lipid and SP-A−Mini-B interactions gave rise to a surprising result. While 1D ^{1}H NMR spectra of SP-A in water displayed the broad and weak peaks expected for a protein the size of an SP-A octadecamer, when micelles were added, the spectra of SP-A changed completely (Figure 1). In the presence of micelles, the spectra of SP-A exhibited relatively intense, resolved, and dispersed peaks, typical of a much smaller protein than an SP-A octadecamer. To estimate the size of the protein complex consistent with these NMR spectra, we calculated the expected line width and intensity (which depend on the rotational correlation time and hence size) for different oligomeric forms of SP-A (Supporting Information, Table S4). For example, the expected line width for an SP-A monomer would be ∼11 Hz as opposed to ∼147 Hz for an octadecamer, and the signal intensity of a monomer would be ∼14 times greater than that for an octadecamer. Thus, the appearance of the SP-A spectra in SDS and DPC micelles are consistent with a complex in the size range of an SP-A monomer to trimer. Also, even though the spectra of SP-A in LMPC, LMPG, and LMPC+LMPG micelles appear to originate from a somewhat larger complex compared to the spectra of SP-A in SDS and DPC micelles, they are still consistent with a micelle-bound SP-A substantially smaller than an octadecamer.

To quantify the oligomeric states of the micelle-bound SP-A, we employed DOSY NMR techniques to obtain translational diffusion measurements. DOSY experiments can reflect a variety of parameters, including the fractions of free and bound species, crowding, shape, and, most prominently, the size. In general, the observed single component diffusion coefficient of a micelle sample corresponds to the weighted average of free and bound species when the rate of exchange is fast on the NMR time scale.[45] Separate diffusion measurements from SDS/DPC and protein peaks for the protein−micelle samples (facilitated by the use of deuterated detergents) allowed us to calculate the fraction of micelles forming complexes with the proteins. In terms of the potential crowding effects, although the particles can experience obstructed diffusion at high concentrations (e.g., ≥100 mM SDS),[49] these were not expected to affect the data at the relatively low concentrations employed for this study (≤50 mM detergent/lipid). While the particle shape indeed affects translational diffusion, the effects of shape changes are small compared to changes in size. For example, ellipsoidal particles 5 times as long as they are wide diffuse only 25% more slowly than spherical particles of the same size.[50] Furthermore, unlike rotational diffusion measurements, translational diffusion measurements are not affected by changes in protein flexibility.[50] We have thus chosen to focus our interpretation of the DOSY data largely on the complex size. For this reason, and because the particle diameter is more intuitive to grasp than the diffusion coefficient, we have converted the diffusion coefficient (D_C) to the apparent hydrodynamic diameter (d_{HA}), i.e., the diameter of a sphere apparently diffusing at the same rate, using the Stokes−Einstein equation.

Diffusion measurements demonstrate that d_{HA} for micelles of all compositions increase substantially upon addition of SP-A, reflecting the formation of detergent/lipid−protein complexes (Table 1 and Figure 6). An analysis based on a two-site model (Supporting Information, Table S1)[45] indicates that, for SDS and DPC systems, more than three-fourths of the micelles are involved in the formation of complexes with SP-A. Interestingly, the d_{HA} for SP-A−SDS and SP-A−DPC complexes are more than 3 times smaller than that for SP-A alone in the absence of micelles. However, for SP-A in complex with LMPC, LMPG, or LMPC+LMPG micelles, the d_{HA} are similar to that of SP-A alone in water. To interpret what this means in terms of the oligomeric state of SP-A within various micelles, we have estimated the contribution of the micelle itself to the diffusion of the complex and used this to estimate the oligomeric state of the SP-A within the micelle−SP-A complex. This analysis indicates SP-A oligomeric states of approximately 10, 12, and 9 molecules in LMPC, LMPG, and LMPC+LMPG micelles, respectively, as well as oligomeric states of approximately 1 and 3 molecules in DPC and SDS micelles, respectively (Supporting Information, Table S5). In the absence of micelles, the diffusion measurements indicate an oligomeric state of even larger than octadecamer (18 molecules) for SP-A. Comparison of SP-A's NMR signal intensity with that of Mini-B (Supporting Information, Table S3) indicates that the vast majority of SP-A molecules, if not the full population, are observed in the NMR spectra acquired in the presence of micelles; i.e., the observed signals are not generated by just a small subpopulation of SP-A. There is, therefore, a dramatic reduction in SP-A's oligomeric state when the protein is bound to micelles.

Presumably, not all of the monomers in the supramolecular SP-A assembly are covalently attached by disulfide bonds; rather,

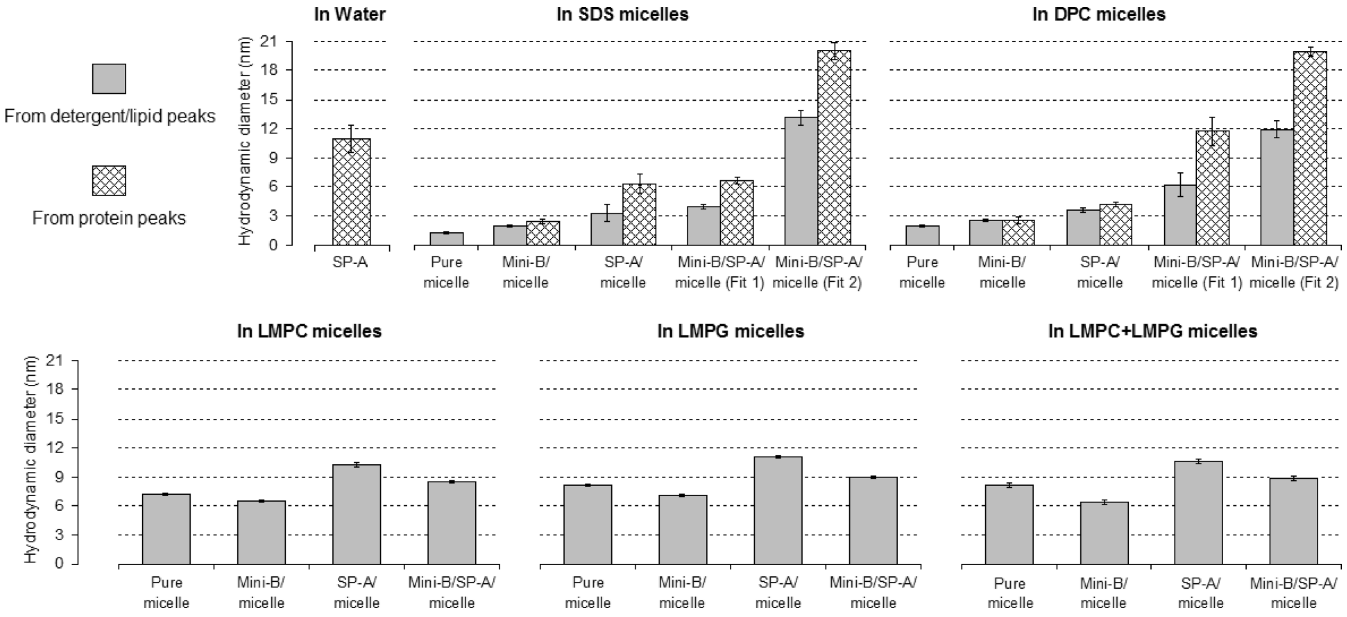

Figure 6. Comparison of the average apparent hydrodynamic diameters (d_{HA}) of SP-A in water, pure micelles, individual SP-A− and Mini-B−micelle complexes, and combined SP-A−Mini-B−micelle complexes as calculated from the 2D DOSY NMR spectra.

many of the subunits are associated only through noncovalent interchain interactions. The addition of amphipathic lipids/detergents appears to disrupt these noncovalent interactions and thus cause the subunits to dissociate. It is plausible that the electrostatic interactions, and perhaps the hydrophobic interactions as well, between the protein and the lipid/detergent molecules overwhelm many of SP-A's intersubunit noncovalent interactions, and thus micelle complexes containing smaller SP-A oligomers are formed.

While micelles provide a surface of higher curvature when compared to the planar surface of lipid bilayers, SP-A's interactions with curved surfaces are probably just as relevant as its interactions with flat surfaces, given that many current models of surfactant mechanisms show SP-A located at the highly curved corners of tubular myelin.[2] Additionally, for membrane proteins where crystal structures have been determined in complex with lipids/detergents, these structures have been found to correspond well with micelle-bound solution structures (e.g., ref 51). It is thus likely, as in micelles, smaller oligomers of SP-A are also present in native lipid environments.

Formation of smaller oligomeric forms when SP-A is bound to micelles has consequences on our understanding of SP-A's functional mechanism, since SP-A's biological roles, in relation to either antimicrobial activities or surfactant biophysical activities, are almost always attributed to its octadecameric structure.[2,17,19] This presumption derives from gel filtration and sedimentation equilibrium studies[52] as well as transmission electron microscopy (TEM)[53] performed with purified SP-A in lipid-free aqueous solutions. However, gel filtration and sucrose density gradient centrifugation of unpurified SP-A have indicated that the protein does not exist purely as fully assembled octadecamers but is consistently found in smaller oligomeric forms including a tetramer of trimers (i.e., 12 molecules), dimer of trimers (i.e., 6 molecules), dimer (i.e., 2 molecules), and even monomer (i.e., a single molecule).[54] The TEM image of recombinant SP-A by itself also displays smaller aggregates like tetramers, trimers and dimers, and even monomers under mild reducing conditions.[53] The TEM image of tubular myelin, on the other hand, shows "X"-shaped structures in the square lattice regions which are modeled as SP-A octadecamers.[2,8] However, on the basis of the data present in this work, as well as in studies such as in ref 54, it appears that it may be time to re-examine the assumption that SP-A functions primarily as an octadecamer.

These studies also reveal several aspects of Mini-B−lipid interactions. First, as indicated by differences in the HSQC spectra of Mini-B (Figure 4), the loop connecting Mini-B's two helices appears to take on a relatively stable conformation in anionic and mixed micelles but undergoes conformational exchange at an intermediate rate in zwitterionic micelles. Second, the DOSY data (Table 1 and Figure 6) indicate that while complexes of Mini-B with SDS and DPC micelles are larger than the micelles alone, the inclusion of Mini-B actually leads to a decrease in d_{HA} of the micelles composed of LMPC, LMPG, and LMPC+LMPG. The most likely explanation for this is that Mini-B induces the formation of micelles with a smaller number of lipids per micelle or causes the micelles to compactify. However, it is also possible that Mini-B causes the micelles to become more spherical. This ability of Mini-B to modulate highly curved lipid structures is of importance in the consideration of the mechanism of its parent protein, SP-B, which is frequently postulated to act by promoting or modifying curved lipid structures.[55,56] The differences observed between Mini-B's effects on the small detergent micelles of SDS and DPC versus its effects on the larger lipid micelles of LMPC, LMPG, and LMPC+LMPG underline that the protein−lipid interactions are governed by factors much more subtle than just the electrostatic charge of the headgroups.

The NMR data provide no indication of any direct interaction between SP-A and Mini-B, which would, for example, have been supported by an SP-A-induced change in the chemical shifts of Mini-B's HSQC peaks (Figure 4). However, there is indeed evidence of SP-A−Mini-B interactions mediated by the micelles. In zwitterionic micelles, Mini-B demonstrates a strong preference to bind SP-A-containing micelles, despite a large excess of SP-A-free micelles (Figure 4G,H). Furthermore, the DOSY data

indicate SP-A−Mini-B interactions in all the micelle systems. For example, with micelles composed of LMPC, LMPG, and LMPC+LMPG, the apparent hydrodynamic diameter of the SP-A−Mini-B−micelle complex is larger than the Mini-B−micelle complex but smaller than the SP-A−micelle complex (Table 1 and Figure 6). This may indicate some potentially interesting effects of Mini-B on SP-A's oligomeric form in LMPC, LMPG, and LMPC+LMPG micelles. Also, at least two distinct size populations of SP-A−Mini-B complexes are found in SDS and DPC micelles. In DPC, both subpopulations are larger in size than individual protein−micelle complexes. In SDS, though one subpopulation is larger, the other one is similar to the size of SP-A−SDS complex. Therefore, perhaps, the entire populations of SP-A and Mini-B interact in the presence of DPC micelles but only subpopulations of the proteins interact in the presence SDS micelles. It is possible that the anionic detergent/lipid molecules of anionic or mixed micelles saturate the cationic sites of the remaining noninteracting Mini-B subpopulation that would otherwise participate in interactions with the anionic sites of SP-A.

In summary, our work demonstrates the need to revisit the frequently encountered assumption that SP-A functions as an octadecamer, since it appears that its lung lipid mimetic micelle-associated configuration is a smaller oligomeric form. Additionally, we provide evidence for lipid-mediated SP-A−SP-B interactions, which likely contribute to normal lung surfactant function, and for the ability of SP-B's structure to be modified by the composition of lipids with which it interacts. That these behaviors are found to be modified in micelles composed of different species but with the same charge underlines the importance of considering subtleties of protein−lipid interactions, beyond just the electrostatic charge of the lipid headgroups.

■ ASSOCIATED CONTENT

Supporting Information. Estimation of free and protein-bound micelle fractions; estimation of hydrodynamic diameters for the SP-A−micelles complexes; comparison of the NMR signal intensities of SP-A + Mini-B with Mini-B; prediction of NMR parameters for different oligomeric forms of SP-A; estimation of masses and oligomeric forms of micelle-bound SP-A; Tables S1−S5. This material is available free of charge via the Internet at http://pubs.acs.org.

■ AUTHOR INFORMATION

Corresponding Author

*Phone (709) 864-4523. Fax (709) 864-2422. E-mail vbooth@mun.ca.

Funding Sources

This research was supported by a CIHR Operating Grant to V.B.

■ ACKNOWLEDGMENT

We are particularly grateful to Dr. Alan Waring for providing the synthetic Mini-B and Mr. Ray Bishop for supplying the cow lungs.

■ ABBREVIATIONS

SP-A, surfactant protein A; SP-B, surfactant protein B; SP-C, surfactant protein C; CRD, carbohydrate recognition domain; NMR, nuclear magnetic resonance; SDS, sodium dodecyl sulfate; DPC, dodecylphosphocholine; LMPC, lysomyristoylphosphatidylcholine; LMPG, lysomyristoylphosphatidylglycerol; DPPC, dipalmitoylphosphatidylcholine; DPPG, dipalmitoylphosphatidylglycerol; SDS-PAGE, sodium dodecyl sulfate−polyacrylamide gel electrophoresis; MALDI-TOF, matrix-assisted laser desorption/ionization−time-of-flight; HPLC, high-performance liquid chromatography; DSS, 2,2-dimethyl-2-silapentane-5-sulfonate; DOSY, diffusion-ordered spectroscopy; PFG, pulsed field gradient; D_C, diffusion coefficient; d_{HA}, apparent hydrodynamic diameter; TEM, transmission electron microscopy.

■ REFERENCES

(1) Sueishi, K., and Benson, B. J. (1981) Isolation of a major apolipoprotein of canine and murine pulmonary surfactant. Biochemical and immunochemical characteristics. *Biochim. Biophys. Acta 665*, 442–453.

(2) Casals, C., and Garcia-Verdugo, I. (2005) Molecular and functional properties of surfactant protein A in *Lung Surfactant Function and Disorder* (Nag, K., and Lenfant, C., Eds.) pp 59−86, Taylor & Francis Group, Boca Raton, FL.

(3) Crouch, E., and Wright, J. R. (2001) Surfactant proteins A and D and pulmonary host defense. *Annu. Rev. Physiol. 63*, 521–554.

(4) Lawson, P. R., and Reid, K. B. (2000) The roles of surfactant proteins A and D in innate immunity. *Immunol. Rev. 173*, 66–78.

(5) Kuroki, Y., Takahashi, M., and Nishitani, C. (2007) Pulmonary collectins in innate immunity of the lung. *Cell. Microbiol. 9*, 1871–1879.

(6) Wright, J. R. (2005) Immunoregulatory Functions of Surfactant Proteins. *Nat. Rev. Immunol. 5*, 58–68.

(7) Haagsman, H. P., and Diemel, R. V. (2001) Surfactant-associated proteins: function and structural variation. *Comp. Biochem. 129*, 91–108.

(8) Nag, K., Munro, J. G., Hearn, S. A., Rasmusson, J., Petersen, N. O., and Possmayer, F. (1999) Correlated atomic force and transmission electron microscopy of nanotubular structures in pulmonary surfactant. *J. Struct. Biol. 126*, 1–15.

(9) Hawgood, S., Bensen, B. J., Schilling, J., Damm, D., Clements, J. A., and White, R. T. (1987) Nucleotide and amino acid sequences of pulmonary surfactant protein SP 18 and evidence for cooperation between SP 18 and SP 28−36 in surfactant lipid adsorption. *Proc. Natl. Acad. Sci. U.S.A. 84*, 66–70.

(10) Schurch, S., Possmayer, F., Cheng, S., and Cockshutt, A. M. (1992) Pulmonary SP-A enhances adsorption and appears to induce surface sorting of lipid extract surfactant. *Am. J. Physiol. 263*, L210–L218.

(11) King, R. J., Carmichael, M. C., and Horowitz, P. M. (1983) Reassembly of lipid-protein complexes of pulmonary surfactant. Proposed mechanism of interaction. *J. Biol. Chem. 258*, 10672–10680.

(12) Hawgood, S., Benson, B. J., Jr., and Hamilton, R. L. (1985) Effects of a surfactant-associated protein and calcium ions on the structure and surface activity of lung surfactant lipids. *Biochemistry 24*, 184–190.

(13) Ikegami, M., Korfhagen, T. R., Whitsett, J. A., Bruno, M. D., Wert, S. E., Wada, K., and Jobe, A. H. (1998) Characteristics of surfactant from SP-A-deficient mice. *Am. J. Physiol. 275*, L247–L254.

(14) Cockshutt, A. M., Weitz, J., and Possmayer, F. (1990) Pulmonary surfactant-associated protein A enhances the surface activity of lipid extract surfactant and reverses inhibition by blood proteins *in vitro*. *Biochemistry 29*, 8424–8429.

(15) Bridges, J. P., Davis, H. W., Damodarasamy, M., Kuroki, Y., Howles, G., Hui, D. Y., and McCormack, F. X. (2000) Pulmonary surfactant proteins A and D are potent endogenous inhibitors of lipid peroxidation and oxidative cellular injury. *J. Biol. Chem. 275*, 38848–38855.

(16) Sanchez-Barbero, F., Strassner, J., Garcia-Canero, R., Steinhilber, W., and Casals, C. (2005) Role of the degree of oligomerization in the structure and function of human surfactant protein A. *J. Biol. Chem. 280*, 7659–7670.

(17) McCormack, F. X. (1998) Structure, processing and properties of surfactant protein A. *Biochim. Biophys. Acta 1408*, 109–131.

(18) Haagsman, H. P., White, R. T., Schilling, J., Lau, K., Benson, B. J., Golden, J., Hawgood, S., and Clements, J. A. (1989) Studies of the structure of lung surfactant protein SP-A. *Am. J. Physiol. 257*, L421–L429.

(19) Kishore, U., Greenhough, T. J., Waters, P., Shrive, A. K., Ghai, R., Kamran, M. F., Bernal, A. L., Reid, K. B. M., Madan, T., and Chakraborty, T. (2006) Surfactant proteins SP-A and SP-D: Structure, function and receptors. *Mol. Immunol. 43*, 1293–1315.

(20) Weaver, T. E. (1988) Pulmonary surfactant-associated proteins. *Gen. Pharmacol. 19*, 361–368.

(21) Palaniyar, N., Ikegami, M., Korfhagen, T., Whitsett, J., and McCormack, F. X. (2001) Domains of surfactant protein A that affect protein oligomerization, lipid structure and surface tension. *Comp. Biochem. Physiol., Part A: Mol. Integr. Physiol. 129*, 109–127.

(22) Head, J. F., Mealy, T. R., McCormack, F. X., and Seaton, B. A. (2003) Crystal structure of trimeric carbohydrate recognition and neck domains of surfactant protein A. *J. Biol. Chem. 278*, 43254–43260.

(23) Weaver, T. E., and Whitsett, J. A. (1991) Function and regulation of expression of pulmonary surfactant-associated proteins. *Biochem. J. 273*, 249–264.

(24) Waring, A. J., Walther, F. J., Gordon, L. M., Hernandez-Juviel, J. M., Hong, T., Sherman, M. A., Alonso, C., Alig, T., Braun, A., Bacon, D., and Zasadzinski, J. A. (2005) The role of charged amphipathic helices in the structure and function of surfactant protein B. *J. Pept. Res. 66*, 364–374.

(25) Nogee, L. M., Garnier, G., Dietz, H. C., Singer, L., Murphy, A. M., deMello, D. E., and Colten, H. R. (1994) A mutation in the surfactant protein B gene responsible for fatal neonatal respiratory disease in multiple kindreds. *J. Clin. Invest. 93*, 1860–1863.

(26) Clark, J. C., Wert, S. E., Bachurski, C. J., Stahlman, M. T., Stripp, B. R., Weaver, T. E., and Whitsett, J. A. (1995) Targeted disruption of the surfactant protein B gene disrupts surfactant homeostasis, causing respiratory failure in newborn mice. *Proc. Natl. Acad. Sci. U.S.A. 92*, 7794–7798.

(27) Korfhagen, T. R., Bruno, M. D., Ross, G. F., Huclsman, K. M., Ikegami, M., Jobe, A. H., Wert, S. E., Stripp, B. R., Morris, R. E., Glasser, S. W., Bachurski, C. J., Iwamoto, H. S., and Whitsett, J. A. (1996) Altered surfactant function and structure in SP-A gene targeted mice. *Proc. Natl. Acad. Sci. U.S.A. 93*, 9594–9599.

(28) Rodriguez-Capote, K., Nag, K., Schürch, S., and Possmayer, F. (2001) Surfactant protein interactions with neutral and acidic phospholipid films. *Am. J. Physiol. Lung Cell. Mol. Physiol. 281*, L231–L242.

(29) Poulain, F. R., Allen, L., Williams, M. C., Hamilton, R. L., and Hawgood, S. (1992) Effects of surfactant apolipoproteins on liposome structure: implications for tubular myelin formation. *Am. J. Physiol. Lung Cell. Mol. Physiol. 262*, L730–L739.

(30) Poulain, F. R., Nir, S., and Hawgood, S. (1996) Kinetics of phospholipid membrane fusion induced by surfactant apoproteins A and B. *Biochim. Biophys. Acta 1278*, 169–175.

(31) Morrow, M. R., Temple, S., Stewart, J., and Keough, K. M. W. (2007) Comparison of DPPC and DPPG environments in pulmonary surfactant models. *Biophys. J. 93*, 164–175.

(32) Venkitaraman, A. R., Hall, S. B., Whitsett, J. A., and Notter, R. H. (1990) Enhancement of biophysical activity of lung surfactant extracts and phospholipid-apoprotein mixtures by surfactant protein A. *Chem. Phys. Lipids 56*, 185–194.

(33) Suzuki, Y., Fujita, Y., and Kogishi, K. (1989) Reconstitution of tubular myelin from synthetic lipids and proteins associated with pig pulmonary surfactant. *Am. Rev. Respir. Dis. 140*, 75–81.

(34) Williams, M. C., Hawgood, S., and Hamilton, R. L. (1991) Changes in lipid structure produced by surfactant proteins SP-A, SP-B, and SP-C. Am. *J. Respir. Cell. Mol. Biol. 5*, 41–50.

(35) Young, S. L., Fram, E. K., and Larson, E. W. (1992) Three-dimensional reconstruction of tubular myelin. *Exp. Lung Res. 18* (4), 497–504.

(36) Sarker, M., Waring, A. J., Walther, F. J., Keough, K. M. W., and Booth, V. (2007) Structure of Mini-B, a Functional Fragment of Surfactant Protein B, in Detergent Micelles. *Biochemistry 46*, 11047–11056.

(37) Gao, G., Williams, J. G., and Campbell, S. L. (2004) Protein-Protein Interaction Analysis by Nuclear Magnetic Resonance Spectroscopy. *Met. Mol. Biol. 261*, 79–91.

(38) Taneva, S., McEachren, T., Stewart, J., and Keough, K. M. W. (1995) Pulmonary surfactant protein SP-A with phospholipids in spread monolayers at the air-water interface. *Biochemistry 34*, 10279–10289.

(39) Haagsman, H. P., Sargeant, T., Hauschka, P. V., Benson, B. J., and Hawgood, S. (1990) Binding of calcium to SP-A, a surfactant-associated protein. *Biochemistry 29*, 8894–8900.

(40) Liu, M., Mao, X. A., Ye, C., Huang, H., Nicholson, J. K., and Lindon, J. C. (1998) Improved WATERGATE pulse sequences for solvent suppression in NMR spectroscopy. *J. Magn. Reson. 132*, 125–129.

(41) Grzesiek, S., and Bax, A. (1993) The importance of not saturating water in protein NMR. Application to sensitivity enhancement and NOE measurements. *J. Am. Chem. Soc. 115*, 12593–12594.

(42) Morris, K. F., and Johnson, C. S. (1992) Diffusion-ordered two dimensional nuclear magnetic resonance spectroscopy. *J. Am. Chem. Soc. 114*, 3139–3141.

(43) Tanner, J. E. (1970) Use of the stimulated echo in NMR diffusion studies. *J. Chem. Phys. 52*, 2523–2526.

(44) Sklenar, V., Piotto, M., Leppik, R., and Saudek, V. (1993) Gradient-tailored water suppression for proton-nitrogen-15 HSQC experiments optimized to retain full sensitivity. *J. Magn. Reson. 102*, 241–245.

(45) Stilbs, P. (1982) Fourier transform NMR pulsed-gradient spin-echo (FT-PGSE) self-diffusion measurements of solubilization equilibria in SDS solutions. *J. Colloid Interface Sci. 87*, 385–394.

(46) Orfi, L., Lin, M., and Larive, C. K. (1998) Measurement of SDS micelle-peptide association using ^{1}H NMR chemical shift analysis and pulsed-field gradient NMR spectroscopy. *Anal. Chem. 70*, 1339–1345.

(47) Whitehead, T. L., Jones, L. M., and Hicks, R. P. (2001) Effects of the incorporation of chaps into SDS micelles on neuropeptide-micelle binding: separation of the role of electrostatic interactions from hydrophobic interactions. *Biopolymers 58*, 593–605.

(48) Nilsson, M., Connell, M. A., Davis, A. L., and Morris, G. A. (2006) Biexponential Fitting of Diffusion-Ordered NMR Data: Practicalities and Limitations. *Anal. Chem. 78*, 3040–3045.

(49) Barhoum, S., and Yethiraj, A. (2009) An NMR study of macromolecular aggregation in a model polymer-surfactant solution. *J. Chem. Phys. 132*, 024909.

(50) Marshall, A. G. (1978) *Biophysical Chemistry: Principles, Techniques and Applications*, John Wiley & Sons, New York.

(51) Fernandez, C., Hilty, C., Bonjour, S., Adeishvili, K., Pervushin, K., and Wuthrich, K. (2001) Solution NMR studies of the integral membrane proteins OmpX and OmpA from Escherichia coli. *FEBS Lett. 504*, 173–178.

(52) King, R. J., Simon, D., and Horowitz, P. M. (1989) Aspects of secondary and quaternary structure of surfactant protein A from canine lung. *Biochim. Biophys. Acta 1001*, 294–301.

(53) Voss, T., Eistetter, H., and Schtifer, K. P. (1988) Macromolecular Organization of Natural and Recombinant Lung Surfactant Protein SP 28−36 Structural Homology with the Complement Factor Clq. *J. Mol. Biol. 201*, 219–227.

(54) Hickling, T. P., Malhorta, R., and Sim, R. B. (1998) Human lung surfactant protein A exsits in several different oligomeric states: oligomer size distribution varies between patient groups. *Mol. Med. 4*, 266–275.

(55) Lipp, M. M., Lee, K. Y., Zasadzinski, J. A., and Waring, A. J. (1996) Phase and morphology changes in lipid monolayers induced by SP-B protein and its amino-terminal peptide. *Science 273*, 1196–1199.

(56) Mariya Chavarha, M., Khoojinian, H., Schulwitz, L. E., Biswas, S. C., Rananavare, S. B., and Hall, S. B. (2010) Hydrophobic Surfactant Proteins Induce a Phosphatidylethanolamine to Form Cubic Phases. *Biophys. J. 98*, 1549–1557.

(57) Cavanagh, J., Fairbrother, W. J., Palmer III, A. G., Rance, M., and Skelton, N. J. (2007) *Protein NMR Spectroscopy Principles and Practice*, 2nd ed., Elsevier Academic Press, Burlington, MA.

(58) Rule, G. S., and Hitchens, T. K. (2006) *Fundamentals of Protein NMR Spectroscopy*, Springer, Dordrecht.